STUDY OF ATTENUATION EFFECT OF WATER DROPLETS ON SHOCKWAVES FROM HYDROGEN EXPLOSION

Kotchourko, A.[1], Mohacsi, J.[1], Lelyakin, A.[1], Zhanjie, X.[1], and Jordan, T.[1]
[1] ITES, Karlsruhe Institute of Technology, Kaiserstraße 12, Karlsruhe, 76131, Germany, alexei.kotchourko@kit.edu

ABSTRACT

The increasing demand for renewable energy storage may position hydrogen as one of the major players in the future energy system. However, to introduce such technology, high level of safety must be offered. In particular, for the accident scenarios with combustion or explosion of the unintendedly released hydrogen in partially or fully confined volumes, such as e.g., road tunnel, the effective countermeasures preventing or reducing the risk of equipment damages and person injuries should be established. A mitigation strategy could be the use of existing fire suppression system, which can inject water as a spray. The shock waves resulted from hydrogen explosion could be weakened by the water droplets met on the shock path.

In the presented work an attenuation effect of water droplets presence on the strength of the passing shock was studied. The analysis of the different attenuation mechanisms was performed and estimation of the effect of spray parameters, such as droplet size and spray density, on the shock wave was carried out. For the quantitative evaluation of the attenuation potential, a numerical model for the COM3D combustion code was developed. The novel model for the droplet behavior accounting for the realistic correlations for the fluid (water) particle drag force linked with the corresponding droplet breakup model describing droplet atomization is presented. The model was validated against literature experimental data and was used for the blind simulations of the hydrogen test facility in KIT.

1.0 INTRODUCTION

In many accidental scenarios, released hydrogen is entrapped within structures and cannot escape into the environment, such as in garages or in road tunnels. In case of accidents with hydrogen vehicles in road tunnels, hazard might result from hydrogen explosion, which produces strong shockwaves propagating through the tunnel. A mitigation strategy could be the use of existing fire suppression systems, which can inject a water spray in case of hydrogen detection. On one hand, the generated water cloud can contribute to preventing the possible ignition of the gas mixture, and on the other, the shockwave produced by the explosion might be weakened by the water droplets.

The current work is devoted to the study of mitigation effect of water droplets on shockwaves and was supported by the EU project “HyTunnel-CS”. Based on these results, methodology allowing to estimate whether existing or future fire protection systems can increase the safety of hydrogen vehicles in tunnels was proposed.

The use of water sprays for the mitigation of shock and blast waves offers several advantages. Due to the large heat capacity and latent heat of vaporization of water, water sprays are capable to absorb a large amount of energy. Moreover, water is affordable, environmentally safe to use and provides the potential for being beneficial for fire suppression and blast wave mitigation [1].

Numerous studies examining the effectiveness of water droplets for shock attenuating purposes were carried out during last decades. In Table 1, a brief overview of a number of recent research surveys with some details is presented. The referred studies were performed with droplet diameters ranging from fine mist of 1 μm to 10 μm [2], up to large droplets of 1 mm to 2.5 mm [3]. The size of the droplet cloud varied from 15 cm [4] to 380 cm [5]. The liquid phase concentration varied from very low concentrations of 5 g/m^3 [6] up to high concentrations of 14 kg/m^3 [4]. In experimental investigations the liquid phase

concentration varied with the droplet size. As the droplets always have certain dispersion in sizes, the values presented in Table 1 are averaged.

Table 1. Summary of applied conditions in previous investigations of the attenuation effect of water droplets on shockwaves.

Author and category of study	Ma	Droplet ⌀, µm	Cloud size, m	Liquid phase, kg/m^3	Pressure attenuation, %
Mataradze [5], exp.		15 – 345	1.20 2.60 3.80		20 26 46
Mataradze [7], exp		25 - 400			
Chikhradze [8], exp.		25 – 400	2.00		54 - 58
Chauvin [9], [4], exp.	1.3, 1.5	500	0.15 0.40 0.70	14.0 11.0 10.0	72 75 78
Jourdan [1], exp., comp.	1.1, 1.5, 1.8	120 250 500	0.36 0.45 0.28	0.22 1.40 13.1	negligible 45 65
Mataradze [6], exp.		25 - 400	4.00	0.0051 0.0198 0.0366	22 47 53
Willauer [10], exp.		54		0.07	25 - 43
Ananth [11], comp.		50		0.08	
Hanson [2], exp., comp.		1 – 10			
Resnyansky and Delaney [12], exp.		80 – 90			
Schwer [13], [14], [15], [16] , comp.		10 – 50	0.15, 0.25, 0.50	0.51 – 2.8	
Thomas [17], exp.		113 – 220	3.40		
Wingerden [18] - [19], exp.		40 – 800			
Borisov [3], exp.	1.07–1.3	1000, 2500	1.50	0.25, 0.76, 1.04	

Here in column #1 annotation *exp* is used for experimental studies and *comp* for computational studies.

Chauvin et al. [9], [4] performed experimental investigations of the propagation of planar shockwaves through a two-phase gas-liquid medium. The authors conducted experiments in a vertically oriented, rectangular shock tube. They examined influence of the droplet cloud length, shock Mach number and liquid phase concentration keeping the mean droplet size constant at 500 µm and found that the mitigation effect clearly increases for higher cloud length and concentrations.

Mataradze et al. [6] conducted attenuation experiments with water droplet sizes ranging from 25 µm to 400 µm in a rectangular test duct. The authors examined influence of liquid phase concentration using several concentrations of 5.1 g/m^3, 19.8 g/m^3 and 36.6 g/m^3. The effect of pressure attenuation ranged from 22 % for 5.1 g/m^3 up to 53% for 36.6 g/m^3. Thus, providing an evidence on the existence of a correlation between the attenuation degree and liquid phase concentration. An attenuation coefficient β was defined, so that the pressure reduction in a rectangular duct can be estimated by the exponential function

$$\Delta P_m = \Delta P_b \cdot e^{-\beta} \quad (1)$$

with $0.25 < \beta < 0.76$ for liquid phase concentrations within the range 5.1 g/m^3 ÷ 36.6 g/m^3.

Jourdan et al. [1] performed research both experimentally and numerically in a vertical shock tube with shockwave Mach numbers ranging from 1.1 to 1.8. Droplets of 120 μm, 250 μm and 500 μm in diameter were used. For the diameter of 500 μm the maximum attenuation of 65% was reached with a Ma number of 1.8, while for droplets of 120 μm the effect is negligible. Additionally, Jourdan performed 1D unsteady numerical calculations. Though the calculations reproduced the experiments reasonably well, the authors suggested to improve the physical model regarding accounting for droplet breakup and vaporization. The authors indicated the dependence of the attenuation degree on the several parameters, including the total droplet volume, the droplet diameter, the shockwave Mach number, which could be grouped in the dimensionless term depending on We and Re numbers.

Schwer and Kailasanath [14], [15], [13], [16] simulated the attenuation effect of shockwaves by water droplets performing Eulerian computations of water mist with droplet diameters of 10 – 50 μm. The results verified a significant attenuation for mass concentrations from 30% to 70%. The computations suggested the momentum absorption from the gas phase by the droplets to be the dominating mechanism of suppression. However, the authors assumed the droplets to remain intact at the shock front, so no droplet breakup was considered.

Ananth et al. [11] conducted calculations using a Lagrangian model to track the breakup and the evaporation of the droplets. For the used liquid phase concentrations of 80 g/m^3, they observed that the child drops evaporate at 100 times higher rate than the parent drops and concluded the latent heat absorption is the dominant mechanism for strong shockwaves.

Igra et al. [20] published a review of methods to attenuate shockwaves. They compared the usage of water droplets with the dust particles and water shields and concluded that utilization of water can be a feasible and suitable option in many cases. Summarizing the literature findings, it can be stated that the degree of attenuation increases with larger droplets, higher liquid phase concentration and larger droplet clouds, however the relation between the shock strength and attenuation effect is still not understood.

2.0 INTERACTION OF SHOCK WITH DROPLETS

When a shockwave hits a droplet, a number of events affecting the shock can occur:

- droplet accelerates by absorbing some of the momentum;
- part of the wave is reflected from the droplet surface and propagates into opposite direction;
- droplet absorb heat from the moving gase (convective heat/thermal radiation, sensible/latent heat);
- droplet fragments due to shear forces in the post-shock flow, the required energy to increase the total droplet surface area (or total surface energy) is transferred from the gas phase to the droplet [11].

The droplet accelerates due to drag force of the flow behind the shock front and pressure differences across the droplet diameter. The momentum, that the acceleration of the droplets requires, decreases the momentum of the shockwave equally, thereby reducing wave strength. Jourdan in [1] and Schwer and Kailasanath in [13] - [16] supposed that the momentum absorption by the droplets is the dominating mechanism of wave weakening.

The maximum possible momentum transfer from moving flow to droplet can be estimated using momentum conservation while assuming the equality of gas and droplet speed at the final state. The momentum transfer coefficient ζ_{max} for the equilibrium velocity u_{eq} then reads as

$$\zeta_{max} = 1 - \frac{u_{eq}}{u_g} = 1 - \frac{\rho_g}{\rho_g + c}, \tag{2}$$

here u_g is initial gas speed, ρ_g is gas density and c is liquid phase mixture density. Note; that high liquid phase mixture density c leads to a high momentum transfer $\zeta \rightarrow 1$, thus being the only parameter, which

determines the maximum momentum exchange. This maximum is reached asymptotically, assuming that drag force acts infinitely long. For the time τ the transfer coefficient can be evaluated as

$$\zeta = \frac{m_d N u(\tau)}{\rho_g \cdot u_g}, \tag{3}$$

here m_d is droplet mass; $u(\tau)$ is velocity which droplet obtained in time τ; and N is volumetric density of droplets. For the conditions of the experiment discussed in the flowing section, the value of transfer coefficient reaches 33.5%. At the same time, the input into the momentum transfer due to pressure difference along the droplet for the same conditions is only ~0.1%.

Jourdan [1] described the large heat capacity and heat of vaporization of water as one of the main advantages using water droplets for blast mitigation. However simple assessment for the droplet in the mentioned flow gives temperature change for gas of 2.7 K and for droplet of 0.9 K.

When the droplet is located in a strong flow, it can deform and fragment to the smaller parts. During droplet break-up event, two stages can be distinguished. In the first stage the droplet deforms, increasing their exchange surface with the gas. In the second stage further deformation leads to the droplet disintegration into two or more smaller parts.

The break-up of the droplet has several consequences on the possible momentum transfer. One clear effect is change of the total liquid surface and corresponding change of the surface energy in the system. Adiga in [21], considered a 500 μm parent droplet fragmenting into 10000 monodispersed child droplets with diameter 23 μm. He has obtained value of 18 J/kg required breakup energy and concluded that the required surface energy for fragmentation is rather negligible compared to the much higher energy of vaporization 2.25 MJ/kg and therefore is not significant in the weakening of shock.

Although this effect is not pronouncedly important, the subsequent breakage of the droplets into the smaller size until reaching unbreakable state, can drastically change the momentum absorption, reflection and heat absorption of the droplets.

3.0 INTACT NUMERICAL DROPLET MODEL

The simulations were performed using the COM3D code developed at the Institute for Thermal Energy Technology and Safety (ITES) in Karlsruhe Institute of Technology.

The model available in the code suitable for droplet simulations is based on the Lagrange particle presentation. The model can represent droplet cloud as an assembly of monodispersed spherical particles with droplets' properties, such as heat capacity and density, corresponding to standard water.

The key issue for the adequate modelling of the interaction with shocks is correct accounting for forces acting on the droplet. The main accelerating force of the droplet is drag force caused by the post-shock flow. The drag force F is proportional to the gas density ρ_g, the cross-sectional area of the droplet A_p, the relative velocity of gas flow and droplet u_{rel} and the dimensionless drag coefficient c_d

$$F = \frac{1}{2} \cdot \rho_g \cdot A_p \cdot c_d \cdot u_{rel}^2. \tag{4}$$

For the wide range of velocities characteristic for the task of shock wave interaction, the drag coefficient cannot be assumed constant due strong violation of the velocity dependence for higher speeds.

A number of studies identified this effect and proposed correlations for the drag coefficient for spheres in a flowing medium depending on the Reynolds number. For the new droplet model, the choice of reliable and physically justified correlation is of primary importance. A set of correlations available in the literature were analyzed.

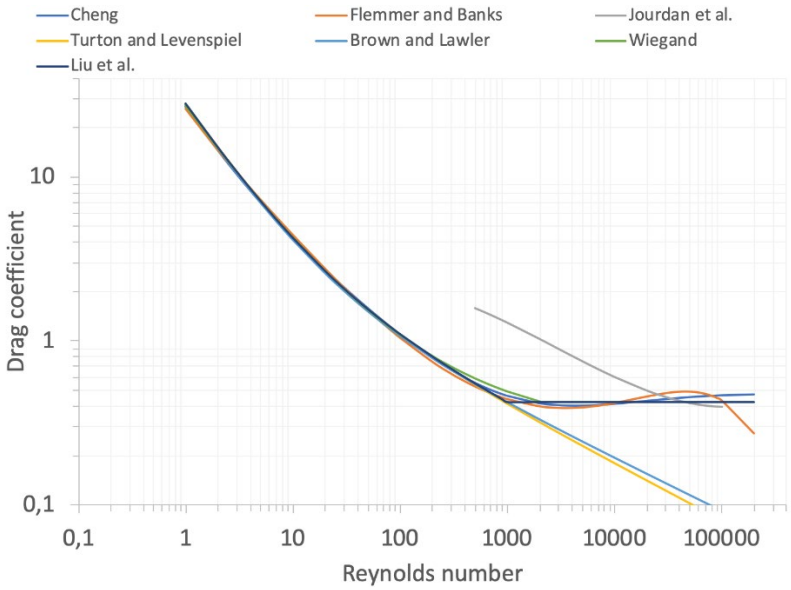

Figure 1. Comparison of different correlations for the drag coefficient as a function of the Reynolds number.

Apparently, with the exception of the Jourdan correlation [21], the behavior of all considered correlations is very similar for Re < 1000 (see Figure 1). In several studies, e.g. in Hongli [22], it was shown that for Reynolds numbers Re > 1000, the drag coefficient remains constant at values of $0.4 < c_d < 0.47$. Other authors, as e.g., Brown and Lawler [23] and Turton and Levenspiel [24] proposed the correlations which disregard this fact. The majority of the authors (Cheng [25], Flemmer and Banks [26], Wiegand [27], Liu [28]) have established the similar characteristics of the proposed dependencies with near constant value for drag coefficient at higher Re. Among these, the correlation of Cheng [25]

$$c_d = \frac{24}{Re} \cdot (1 + 0.27 \cdot Re)^{0.43} + 0.47 \cdot \left(1 - \exp(-0.04 \cdot Re^{0.38})\right) \quad (5)$$

is characterized by the smooth behavior over the whole range of validity and demonstrated accuracy sufficiency to experimental data.

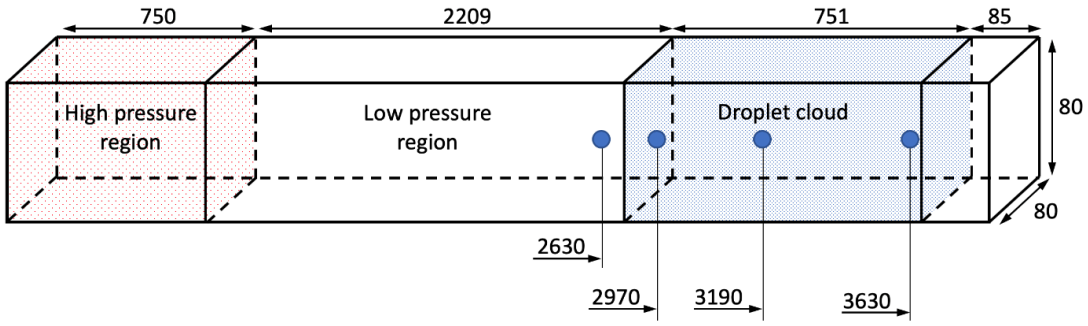

Figure 2. Test site schematic of planar shockwave propagation through a droplet cloud to study attenuation effect on shock pressure [4].

For the validation of the particle model, the experiments conducted by Chauvin et al. (2011) [4] as best corresponding the considered environmental conditions were selected. The schematic of the experimental facility is given in Figure 2. The shockwave in the facility is initiated by relief of the air from high-pressure section. In the simulation the parameters of the high-pressure section (initial pressure 6.75 bar) were adjusted to match the shock in the droplet section with 1.5 Ma referred in the experiment. The droplet cloud was represented by the assembly of water particles with volume fraction of 1%, liquid phase density of 10 kg/m^3, and particle diameter of 500 µm.

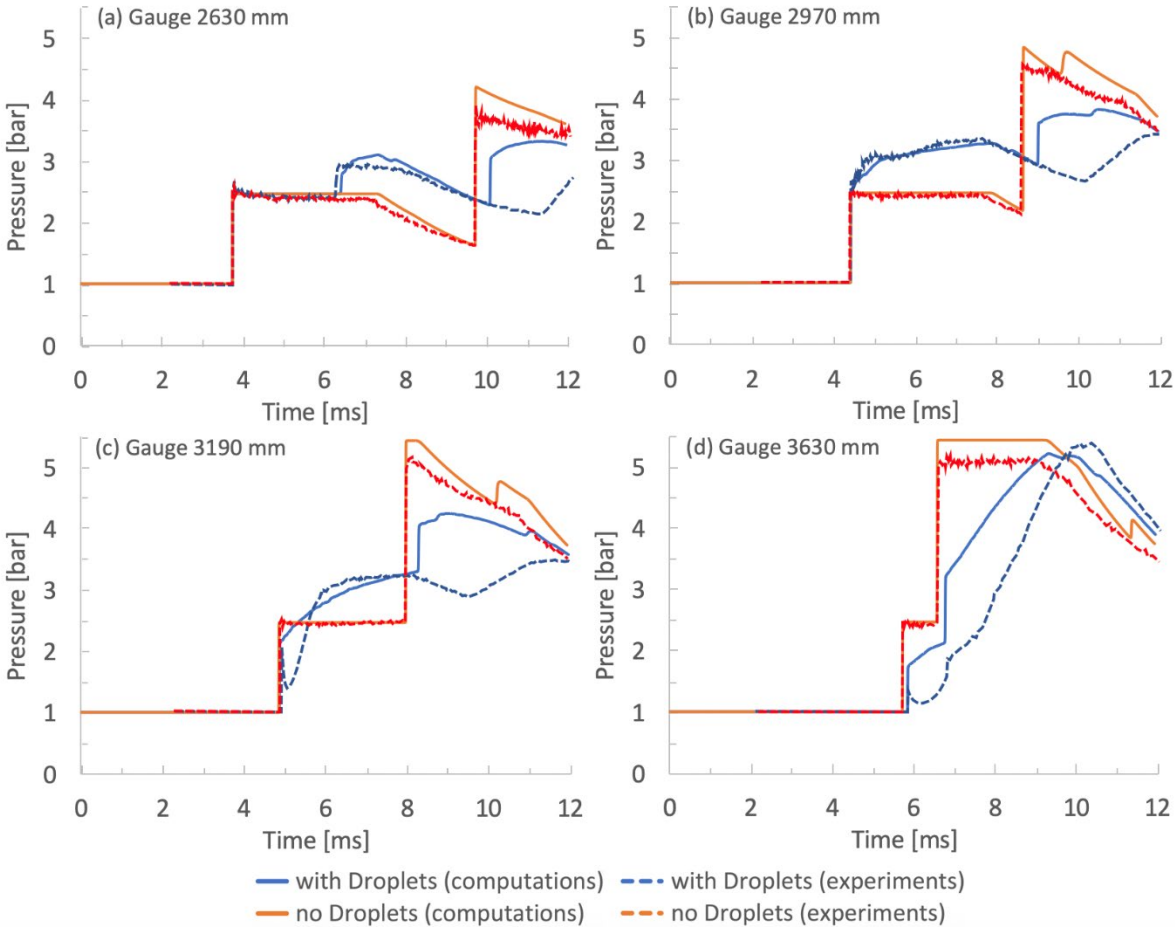

Figure 3. Comparison of the Chauvin test data (2011) [4] and COM3D simulation with model of non-breakable droplets.

In Figure 3 the validation simulation results are presented (solid lines) and compared with the results of the referred experiments [4] (dashed lines). For each of the four gauges shown in Figure 2, the pressure is plotted against the time. The blue curves represent the experiments with droplet cloud in the channel. The red curves are referring to the reference test results, for which the channel is filled only with air.

In general, for all gauges the simulation without droplets (red curves), the results of experiment and simulation agree very well, excluding the later stage, when reflected from the rear wall shock reaches gauges. The discrepancy is connected with disregarded heat loses in the simulation. Thus, without droplets the simulated set up demonstrated ability to reproduce the shockwave propagation accurately.

The first gauge (a) 2630 mm is located in front of the droplet cloud. Naturally, for time less than 6 ms there is no difference in the pressure curves with and without droplets. Up to ~6 ms, also the blue curves (tests with droplets/particles) agree. At t = ~6 ms the blue curve shows the reflection of the shockwave from the front of the droplet cloud. Both the instant of time of the reflection and the amount of the increase are of the same order of magnitude for experiments and simulations. In the simulations with droplets, the pressure increases suddenly again at t = ~10 ms, which can be explained by the rear-wall reflection. In the experiments with droplets, this rear-wall reflection is not visible similarly to all other gauges. The second gauge (b) 2970 mm is located inside the cloud at 20 mm behind the cloud front surface. The total picture of shock propagation is largely similar to the first gauge.

At the third gauge (c) 3190 mm, the clear influence of the droplet presence on the shock parameters can be observed. Both in the experiment and in the calculation, the amplitude diminishing of the shockwave entering the cloud is pronounced. However, the experiment and simulation give different shock front behavior. The experiment shows the characteristic pressure drop after the shockwave has arrived. This effect cannot be reproduced in the tested particle model. The similar observations are even more pronounced in the measurement at the last gauge (d) 3630~mm near the rear front of the cloud.

Note here that possible effect of the influence of liquid phase on the sound speed should be also accounted for. In general, the droplets presence can provide a significant impact on the resulting sound speed of the mixture, see [29] for instance. Meanwhile in the presented simulations only a very small decrease of the shock velocity in presence of the droplets is observed. Therefore, experiments and simulations cannot confirm the predicted influence of the droplets on the speed of sound. The COM3D code can reproduce the shock velocity properly, thus the effect of the liquid on the sound speed is calculated correctly in the simulation.

The difference of the experiment and simulation for two gauges inside droplet cloud together with the observed discrepancy of the rear-wall reflection behavior in first and second gauges gives clear indications for the lack of the accounted features in the tested droplet model. As the possible source for the model improvement, a mechanism of the droplets' fragmentation was analyzed.

4.0 DROPLET BREAK-UP NUMERICAL MODEL

For the numerical modeling of the droplet breakup, three different values have to be known: i) a critical Weber number defining the onset of the breakup; ii) the breakup time necessary for breakup; and iii) a method for evaluation of produced secondary droplets.

For the breakup time, Pilch and Erdman (1987) [30] proposed to distinguish an initial breakup time, a primary breakup time and a total breakup time. The initial breakup time is the time required for the droplet to deform beyond the oblate ellipsoid shape. After the droplet is deformed, the primary breakup occurs within in the primary breakup time. If the total breakup time is sufficiently high, multiple breakups can occur until the total breakup time is reached. When the total breakup time is reached, the fragmentation of the droplet ended .

For the characterization of the breakup process the dimensionless time was introduced by Nicholls and Ranger (1969) [31]

$$t_{char} = \frac{\Phi}{u_{rel}} \sqrt{\frac{\rho_d}{\rho_g}}. \tag{6}$$

For the initial breakup time as $t_{ini} = t_{char} \cdot T^*_{ini}$ different correlations were proposed. Schmehl et al. [32] suggested to use a constant value for $T^*_{ini} = 1.6$ for low viscosity $Oh < 0.1$.

Wolfe and Anderson [33] found that for higher droplet viscosity $Oh > 0.1$ the initiation of breakup occurs delayed. Later, Pilch and Erdman [30] suggested the following correlation for the initial breakup time as a function of Ohnesorge and Weber numbers

$$T^*_{ini} = 1.9(We - 12)^{-0.25}(1 + 2.2Oh^{1.6}); \text{ for } Oh < 1.5. \tag{7}$$

Hsiang and Faeth [34] suggested a correlation only depending on the Ohnesorge number

$$T^*_{ini} = \frac{1.6}{1 - Oh/7}; \text{ for } Oh < 3.5, \tag{8}$$

and earlier another correlation was proposed by Gelfand [35]

$$T^*_{ini} = 1.4(1 + 1.5Oh^{0.74}); \text{ for } Oh < 4. \tag{9}$$

The mentioned four formulas are compared as a function of the Ohnesorge number in Figure 4; for the Pilch and Erdman correlation is used We = 14 as critical value, for higher Weber numbers the function is clearly different.

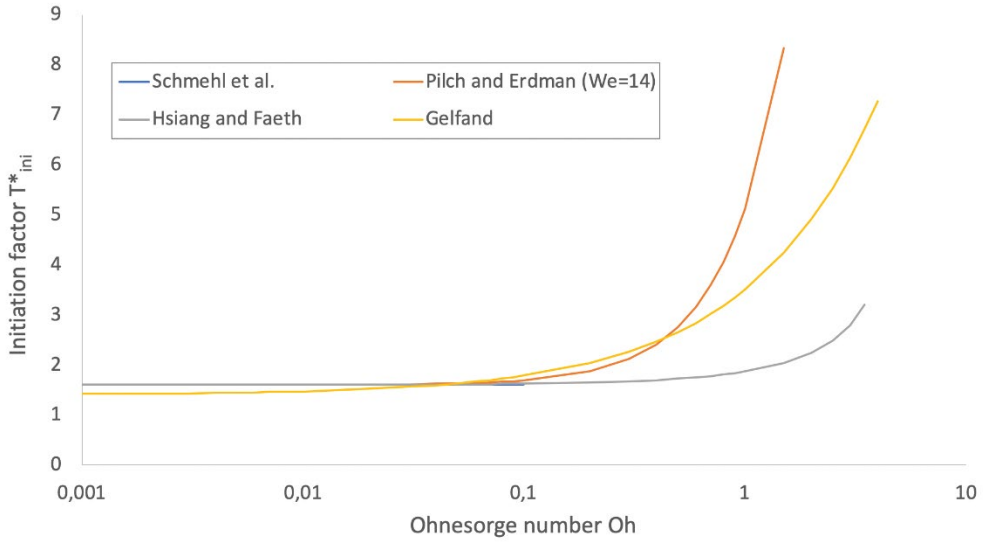

Figure 4. Comparison of initial breakup time models from [32], [30], [34], and [35].

Note, that the constant value assumption for $T^*_{ini} = 1.6$ corresponds to all models for low viscosity Oh < 0.1. For higher Ohnesorge numbers, it is questionable *a priory* to pick out correct dependence. Taking into account that for the conditions of the current work the Ohnesorge number is always small Oh < 0.1, we stick with assumption of constant value of $T^*_{ini} = 1.6$ while using Pilch formula for Oh > 0.1.

For the primary breakup time there is only one correlation found in the literature. Pilch and Erdman [30] suggested to use a constant value for $t_{prim} = t_{char} \cdot 1.25$.

For the total breakup time $t_{tot} = t_{char} \cdot T^*_{tot}$, there were few schemes found in the literature. Pilch and Erdman [30] suggested the following correlation for small Ohnesorge numbers Oh < 0.1.

$$T^*_{tot} = \begin{cases} 6 \cdot (We - 12)^{-0.25}; & 12 \le We < 18 \\ 2.45 \cdot (We - 12)^{0.25}; & 18 \le We < 45 \\ 14.1 \cdot (We - 12)^{-0.25}; & 45 \le We < 351 \\ 0.766 \cdot (We - 12)^{0.25}; & 351 \le We < 2670 \\ 5.5; & 2670 \le We \end{cases} \quad (10)$$

Remark: The third equation has been corrected due to a suggested typographical mistake in the original publication of Pilch and Erdman [30]. Gelfand et al. [35] did not respect the different breakup modes and proposed the following function

$$T^*_{tot} = 4.5(1 + 1.2Oh^{0.74}) \quad \text{for} \quad Oh < 0.3. \quad (11)$$

Hsiang and Faeth [34] developed an additional correlation valid also for higher Ohnesorge numbers

$$T^*_{tot} = \frac{5}{1 - Oh/7} \quad \text{for} \quad Oh < 3.5. \quad (12)$$

The same authors for the evaluation of the secondary droplet size recommended to use function of the primary droplet size accounting for the Ohnesorge number and a corrected Weber number We_{corr}

$$\Phi_{sec} = \Phi \cdot 1.5 \cdot Oh^{0.2} \cdot We_{corr}^{-0.25}. \quad (13)$$

The idea of the Weber number correction to account for viscosity effects for higher Ohnesorge numbers Oh > 0.1 belongs to Schmehl et al. introduced in [32]

$$We_{corr} = \frac{We}{1+1.077Oh^{1.6}}. \quad (14)$$

The proposed model correlations were analyzed and tested against experimental data during validation procedure.

5.0 MODEL TESTING AND VALIDATION

For the testing and validation of the droplet model presented in the previous section, modeling of the Chauvin test channel [4] were performed. In the proposed model, the Pilch and Erdman correlation for total breakup time for Oh < 0.1 and proposal from Gelfand for Oh > 0.1 were used.

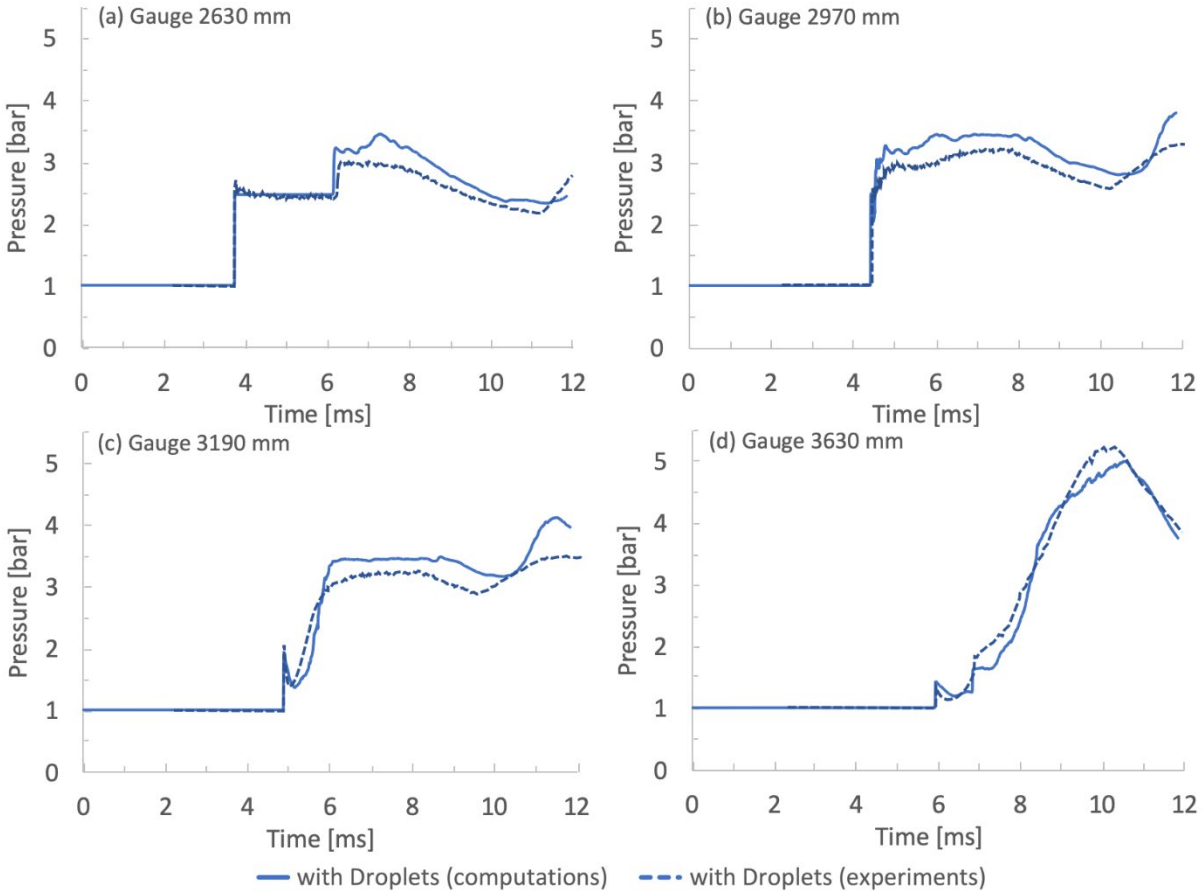

Figure 5. Results of COM3D simulations using the developed droplet breakup model compared with experimental data of Chauvin et al. (2011) [4].

In Figure 5 comparison of the measured and computed pressure curves at four pressure gauge locations are shown. Apparently, accounting for the droplet breakup allowed to match the specific features of the shock propagating through droplet cloud. In particular, at the gauges (c) and (d) the model is able to reproduce the characteristic pressure fall. The amplitude and duration of the pressure descent is defined by the peculiarities of the droplet fragmentation. At the gauge near the rear of the droplet cloud (d), both the shock pressure (at approx. 6 ms) and the delayed maximum pressure (at approx. 10 ms) could be reproduced with small uncertainty.

The excellent agreement for both quantitative and qualitative integral characteristics between experiment and simulation convincingly confirm the correctness of the model details' selection.

In order to check the validity of the model for different test conditions, simulations using the data of Jourdan et al. [1] were performed. The authors of [1] conducted experiments using the same test channel as Chauvin et al., which is illustrated in Figure 2 but applied different pressure gauges and a shock with Mach number of 1.1. Additionally, they performed 1D unsteady numerical calculations. In Figure 6 the results of the current simulations (blue, solid line) with the experimental data (blue, dashed line) and the simulations of Jourdan [1] (orange, dashed) are presented. The comparison demonstrates that shock behavior is reproduced very well. Due to the lower shock velocity, the effect of droplet breakup is less pronounced. At the end of the droplet cloud (gauge (c)), the absolute pressure values agree quite good as well as the time dynamics. The lack of the accurate prediction of Jourdan is highly likely connected with the missing effect of droplet breakup.

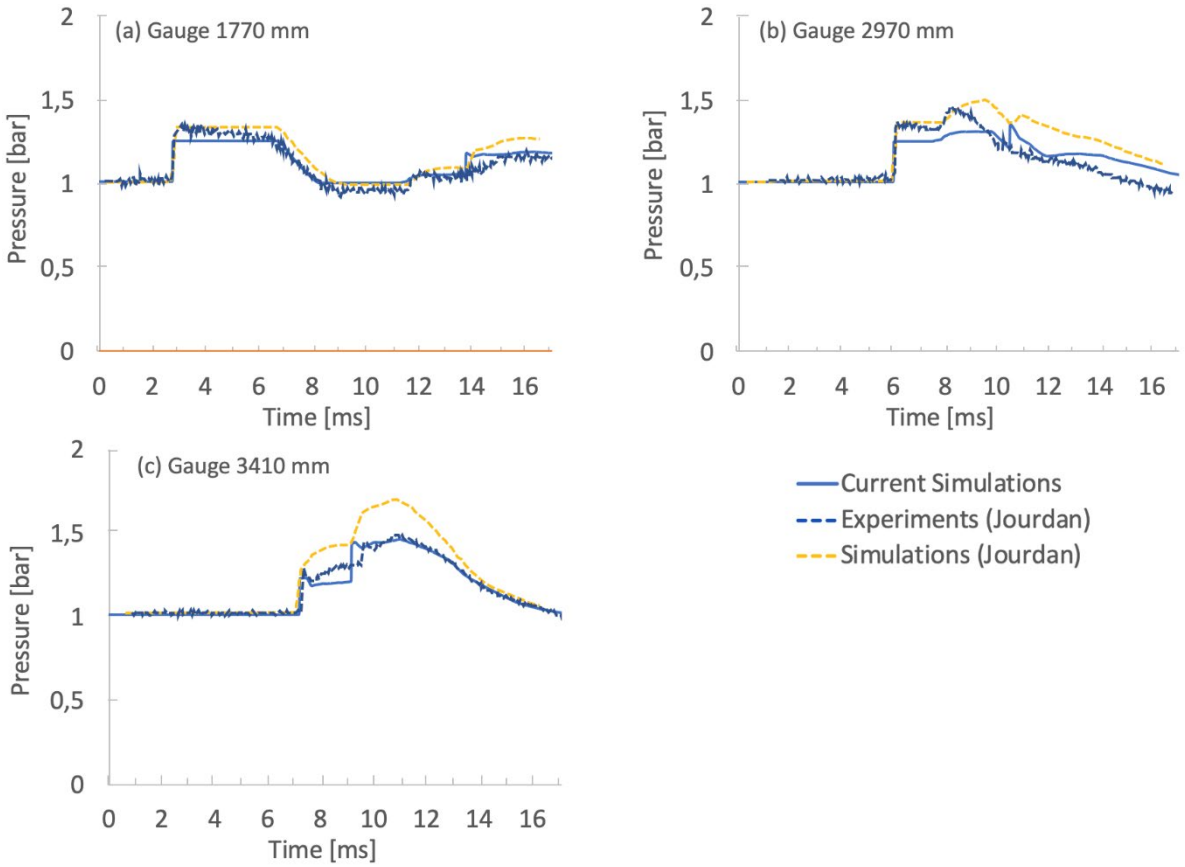

Figure 6. Results of simulations with breakup model compared with experimental data of Jourdan et al. (2010) [1].

Additional efforts to validate the proposed model, were made to prove the solution independence on numerical grid. The simulations were carried out with the conditions of the Chauvin test channel from the previous section. The Figure 7 presents the pressure at the four gauges for mesh resolutions of 1 mm and 5 mm. In general, the curves agree very well. As expected, for the smaller mesh sizes the results are calculated more accurately. There is good agreement of the results in characteristic points, the shock velocity and the amplitude of the pressure are predicted with accuracy which could be expected for the corresponding mesh resolution.

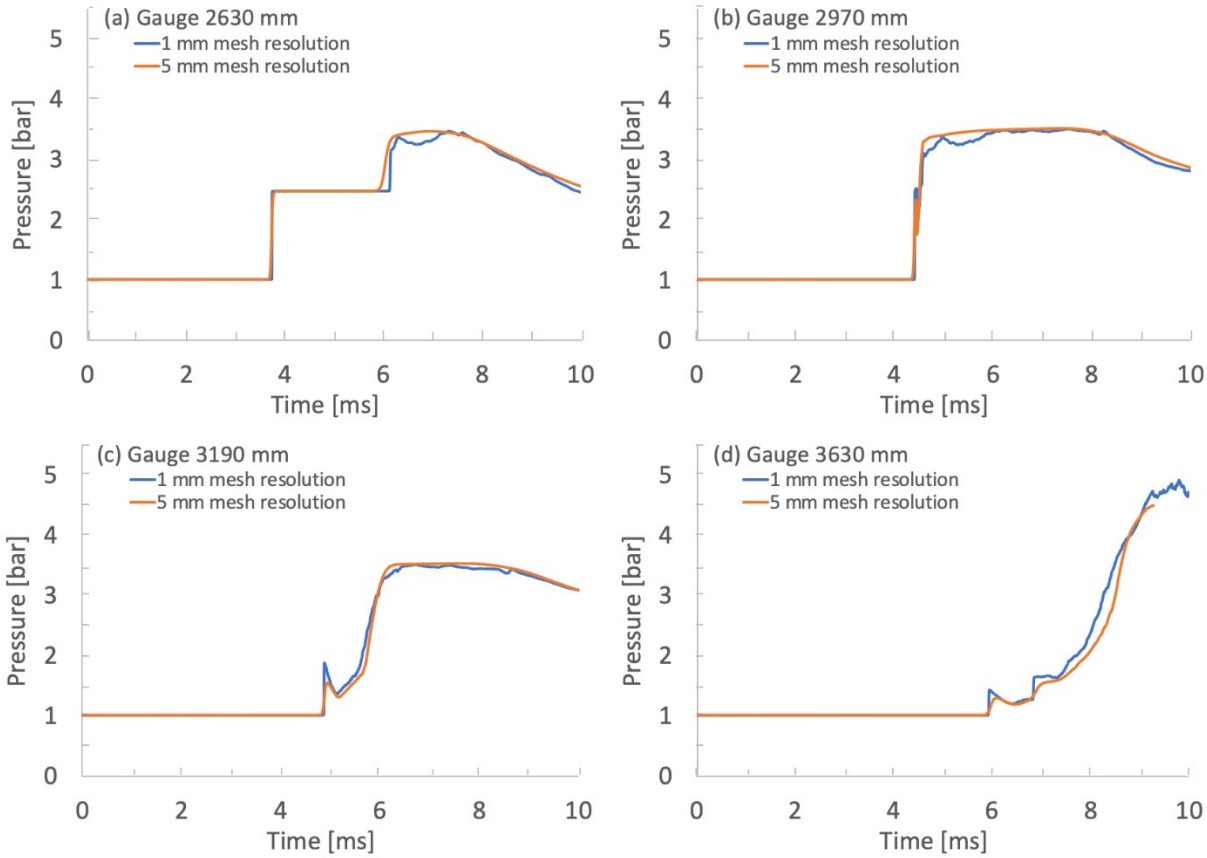

Figure 7. Comparison of the pressure course for simulations with mesh resolution of 1 mm (blue curve) and 5 mm (orange curve).

SUMMARY

A set of possible mechanisms of blast waves attenuation were analyzed based on the literature survey. The absorption of the shockwave momentum by the droplet acceleration and the droplet fragmentation were assessed as the dominant mechanisms of the pressure wave suppression. The liquid phase concentration could be defined as the most important parameter for the shock strength reduction.

For the quantitative estimate of attenuation effect, numerical simulations were performed using comprehensive droplet model which was developed and implemented in the COM3D code. Initially, several candidates describing drag force for the Lagrangian particles were analyzed and compared. Detailed analysis for the fragmentation process was carried out and the corresponding numerical model for the breakup time and the secondary droplet size were implemented and tested.

The newly developed numerical model of interaction between shock wave and water droplets was validated against two sets of experimental data available in the literature. The model demonstrated excellent performance in the relatively wide range of conditions in the droplet cloud and for shock strength.

The developed model was used to analyze possible shock wave attenuation in the water droplet cloud as the mitigation measure for the hydrogen utilizing equipment. As a concluding remark it can be confirmed, that the use of fire suppression systems can be a perspective method for attenuation of strong pressure waves in tunnels; whereas, for the modern mist-based systems the expected effectiveness could be significantly lower than for the older systems due to the smaller liquid phase mixture density of the fine mist.

REFERENCES

[1] G. Jourdan, L. Biamino, C. Mariani, C. Blanchot, E. Daniel, J. Massoni, L. Houas, R. Tosello and D. Praguine, "Attenuation of a shock wave passing through a cloud of water droplets," *Shock Waves,* vol. 20, pp. 285-296, 2010.

[2] T. C. Hanson, D. F. Davidson and R. K. Hanson, "Shock-induced behavior in micron-sized water aerosols," *Physics of Fluids,* vol. 19, p. 056104, 2007.

[3] A. A. Borisov, B. E. Gelfand, S. A. Gubin, S. M. Kogarko and O. V. Krivenko, "Attenuation of shock waves in a two-phase gas-liquid medium," *Fluid Dynamics,* vol. 6, pp. 892-897, 1971.

[4] A. Chauvin, G. Jourdan, E. Daniel, L. Houas and R. Tosello, "Experimental investigation of the propagation of a planar shock wave through a two-phase gas-liquid medium," *Physics of Fluids,* vol. 23, p. 113301, 2011.

[5] E. Mataradze, M. Chikhradze, K. Tavlalashvili, N. Bochorishvili and I. Akhvlediani, "Impact of Water Mist Thickness on Shock Wave Attenuation," *IOP Conference Series: Earth and Environmental Science,* vol. 221, p. 012106, 2019.

[6] E. Mataradze, T. Krauthammer, N. Chikhradze and E. Chagelishvili, "Influence of liquid phase concentration on shock wave attenuation in mist," *International Symposium on Military Aspects of Blast and Shock (MABS),* vol. 21, 2010.

[7] E. Mataradze, N. Chikhradze, N. Bochorishvili, I. Akhvlediani and D. Tatishvili, "Experimental Study of the Effect of Water Mist Location On Blast Overpressure Attenuation in A Shock Tube," *IOP Conference Series: Earth and Environmental Science,* vol. 95, p. 042031, 2017.

[8] N. Chikhradze, E. Mataradze, M. Chikhradze, T. Krauthammer, Z. Mansurov and E. Alyiev, "Methane Explosion Mitigation in Coal Mines by Water Mist," *IOP Conference Series: Earth and Environmental Science,* vol. 95, p. 042029, 2017.

[9] A. Chauvin, G. Jourdan, E. Daniel and C. Mariani, "Investigation of the attenuation of a shock wave passing through a water spray," *International Symposium on Military Aspects of Blast and Shock (MABS) 21,* 2010.

[10] H. D. Willauer, P. Ananth, J. P. Farley and F. W. Williams, "Mitigation of TNT and Destex explosion effects using water mist," *Journal of Hazardous Materials,* vol. 165, pp. 1068-1073, 2009.

[11] R. Ananth, H. Ladouceur, H. Willauer, J. Farley and F. Williams, "Effect of water mist on a confined blast," *Suppression and Detection Research and Applications - A Technical Working Conference,* 2008.

[12] A. D. Resnyansky and T. G. Delaney, "Experimental study of blast mitigation in a water mist," *Defence Science and Technology Organisation Edinburgh (Australia),* 2006.

[13] D. Schwer and K. Kailasanath, "Blast mitigation by water mist (1) simulation of confined blast waves," *Naval Research Laboratory Washington DC,* 2002.

[14] D. Schwer and K. Kailasanath, "Blast Mitigation by Water Mist (2) Shock Wave Mitigation Using Glass Particles and Water Droplets in Shock Tubes," *Naval Research Laboratory Washington DC,* 2003.

[15] D. Schwer and K. Kailasanath, "Blast Mitigation by Water Mist (3) Mitigation of Confined and Unconfined Blasts," *Naval Research Laboratory Washington DC,* 2006.

[16] D. Schwer and K. Kailasanath, "Numerical simulation of the mitigation of unconfined explosion using water-mist," *Proceedings of the Combustion Institut,* vol. 31, pp. 2361-2369, 2007.

[17] G. O. Thomas, "On the Conditions Required for Explosion Mitigation by Water Sprays," *Process Safety and Environmental Protection,* vol. 78, pp. 339-354, 2000.

[18] K. van Wingerden and B. Wilkins, "The influence of water sprays on gas explosions. Part 1: water-spray-generated turbulence," *Journal of Loss Prevention in the Process Industries,* vol. 8, pp. 53-59, 1995.

[19] K. van Wingerden, "Mitigation of gas explosions using water deluge," *Process Safety Progress,* vol. 19, pp. 173-178, 2000.

[20] O. Igra, J. Falcovitz, L. Houas and G. Jourdan, "Review of methods to attenuate shock/blast waves," *Progress in Aerospace Sciences,* vol. 58, pp. 1-35, 2013.

[21] G. Jourdan, L. Houas, O. Igra, J.-L. Estivalezes, C. Devals and E. E. Meshkov, "Drag coefficient of a sphere in a non-stationary flow: new results," *Proceedings of the Royal Society A: Mathematical, Physical and Engineering Sciences,* vol. 463, p. 3323–3345, 2007.

[22] Y. Hongli, M. Fan, A. Liu and L. Dong, "General formulas for drag coefficient and settling velocity of sphere based on theoretical law," *International Journal of Mining Science and Technology,* vol. 25, pp. 219-223, 2015.

[23] P. P. Brown and D. F. Lawler, "Sphere Drag and Settling Velocity Revisited," *Journal of Environmental Engineering,* vol. 129, pp. 222-231, 2003.

[24] R. Turton and O. Levenspiel, "A short note on the drag correlation for spheres," *Powder Technology,* vol. 47, pp. 83-86, 1986.

[25] N.-S. Cheng, "Comparison of formulas for drag coefficient and settling velocity of spherical particles," *Powder Technology,* vol. 189, pp. 395-398, 2009.

[26] R. L. C. Flemmer and C. L. Banks, "On the drag coefficient of a sphere," *Powder Technology,* vol. 48, pp. 217-221, 1986.

[27] H. Wiegand, "Die Einwirkung eines ebenen Strömungsfeldes auf frei bewegliche Tropfen und ihren Widerstandsbeiwert im Reynoldszahlbereich von 50 bis 2000," *Forschung im Ingenieurwesen A,* vol. 54, p. 188–188, 1988.

[28] A. B. Liu, D. Mather and R. D. Reitz, "Modeling the effects of drop drag and breakup on fuel sprays," *SAE Transactions,* p. 83–95, 1993.

[29] K. C. Adiga, H. D. Willauer, R. Ananth and F. W. Williams, "Implications of droplet breakup and formation of ultra fine mist in blast mitigation," *Fire Safety Journal,* vol. 44, pp. 363-369, 2009.

[30] M. Pilch and C. A. Erdman, "Use of breakup time data and velocity history data to predict the maximum size of stable fragments for acceleration-induced breakup of a liquid drop," *International Journal of Multiphase Flow,* vol. 13, pp. 741-757, 1987.

[31] J. A. Nicholls and A. A. Ranger, "Aerodynamic shattering of liquid drops.," *AIAA Journal,* vol. 7, pp. 285-290, 1969.

[32] R. Schmehl, G. Maier and S. Wittig, "CFD Analysis of Fuel Atomization, Secondary Droplet Breakup and Spray Dispersion in the Premix Duct of a LPP Combustor," *Eighth International Conference on Liquid Atomization and Spray Systems, Pasadena, CA, USA,* 2000.

[33] H. E. Wolfe and W. H. Andersen, "Kinetics, mechanism, and resultant droplet sizes of the aerodynamic breakup of liquid drops," 1964.

[34] L.-P. Hsiang and G. M. Faeth, "Near-limit drop deformation and secondary breakup," *International Journal of Multiphase Flow,* vol. 18, pp. 635-652, 1992.

[35] B. E. Gelfand, S. Gubin, S. Kogarko and S. Komar, "Singularities of the breakup of viscous liquid droplets in shock waves," *Journal of Engineering Physics,* vol. 25, pp. 1140-1142, 9 1973.

[36] K. van Wingerden and B. Wilkins, "The influence of water sprays on gas explosions. Part 2: mitigation," *Journal of Loss Prevention in the Process Industries,* vol. 8, pp. 61-70, 1995.

[37] O. Igra, G. Ben-Dor, F. Aizik and B. Gelfand, "Experimental and Numerical Investigation of Shock Wave Attenuation in Dust-Gas Suspensions," *Shock Waves @ Marseille III,* pp. 49-54, 1995.